polysaccharides

Article

Encapsulation of Allergens into Core–Shell Chitosan Microparticles for Allergen-Specific Subcutaneous Immunotherapy

Mariya Konovalova [1], Elena Kashirina [1], Kseniya Beltsova [1,2], Olga Kotsareva [1], Gulnar Fattakhova [1] and Elena Svirshchevskaya [1,*]

[1] Shemyakin & Ovchinnikov Institute of Bioorganic Chemistry, Russian Academy of Sciences GSP-7, 16/10, Miklukho-Maklaya St., 117997 Moscow, Russia; mariya.v.konovalova@gmail.com (M.K.); helen-kas@mail.ru (E.K.); beltsova.kseniya@mail.ru (K.B.); olga.kotsareva@gmail.com (O.K.); gfattakhova@yahoo.com (G.F.)

[2] Institute of Biochemical Technologies and Nanotechnologies, RUDN University, 6, Miklukho-Maklaya St., 117198 Moscow, Russia

* Correspondence: esvir@mail.ibch.ru; Tel.: +7-9104648760

Abstract: IgE-mediated allergic reaction occurs in response to harmless environmental compounds, such as tree and grass pollen, fragments of household microorganisms, etc. To date, the only way to treat IgE-mediated allergy is allergen-specific immunotherapy (ASIT), which consists of a prolonged subcutaneous administration of allergen extracts or recombinant proteins. The long duration of the treatment, the cost and the risk of life-threatening adverse reactions are the main limiting factors for ASIT. The aim of this work was to develop allergen proteins encapsulated in chitosan-based microparticles that can be safely administered at high doses and in a rash protocol. The egg white allergen, Gal d 1 protein, was used as a model antigen. The protein was packed into core–shell type microparticles (MPs), in which the core was formed with succinyl chitosan conjugated to Gal d 1, subsequently coated with a shell formed by quaternized chitosan. The obtained core–shell MPs containing Gal d 1 in the core (Gal-MPs) were non-toxic to macrophage and fibroblast cell lines. At the same time, Gal-MPs were quickly engulfed by bone marrow-derived dendritic cells or RAW264.7 macrophage cells, as was visualized using flow cytometry and confocal microscopy. Encapsulated Gal d 1 was not recognized by Gal d 1-specific IgE in ELISA. Female BALB/c mice were immunized with Gal-MPs subcutaneously three times a week for 2 weeks. Immunization of mice resulted in IgG titers 1250 ± 200 without IgE production. Allergy in control and vaccinated mice was induced by low-dose Gal d 1 injections in the withers of mice. IgE was induced in control-sensitized but not in the vaccinated mice. Thus, preventive vaccination with the encapsulated allergens is safe and rapid; it significantly reduces the risk of IgE production induced by respiratory and oral allergens.

Keywords: succinyl chitosan; quaternized chitosan; encapsulated proteins; subcutaneous immunization

Citation: Konovalova, M.; Kashirina, E.; Beltsova, K.; Kotsareva, O.; Fattakhova, G.; Svirshchevskaya, E. Encapsulation of Allergens into Core–Shell Chitosan Microparticles for Allergen-Specific Subcutaneous Immunotherapy. *Polysaccharides* **2023**, *4*, 142–155. https://doi.org/10.3390/polysaccharides4020011

Academic Editor: Cédric Delattre

Received: 3 March 2023
Revised: 24 April 2023
Accepted: 11 May 2023
Published: 15 May 2023

1. Introduction

IgE-mediated allergy is one of the most common diseases in the world. It occurs in response to harmless non-replicating compounds, such as pollen of trees and grasses, fragments of household microorganisms, food, fungus spores and conidia, etc. Most allergy medications suppress the innate response to allergy mediators, preventing the activation and degranulation of mast cells. To date, the only way to attenuate allergy is allergen-specific immunotherapy (ASIT), which consists of a prolonged subcutaneous administration of small doses of allergen extracts [1] lasting, in some cases, for years. It was shown that ASIT results in IgG4 production, which partially prevents the development of hypersensitivity to the allergens, and slows down the transition to severe forms of allergies, such as bronchial asthma and atopic dermatitis [2]. ASIT vaccines are administered in

small amounts, gradually increasing the doses due to the risk of anaphylactic shock, which makes it difficult to transit from IgE to IgG response.

Allergen extracts for ASIT are complex mixtures of proteins and non-protein compounds containing a large amount of impurities, therefore, side reactions, including an anaphylactic shock may occur [3]. The difficulty in the manufacture of allergen extracts is the need to standardize the composition of ASIT preparations, which varies from batch to batch. To increase the effectiveness of ASIT and reduce the possibility of adverse reactions, the surface structure of allergens can be modified, including chemical modification or encapsulation of allergens in microgranules. Preparations with a modified allergen surface makes ASIT lose its ability to interact with IgE, therefore they can be used in doses many times higher than in the standard protocol [4].

Currently, several possible ASIT mechanisms have been proposed. ASIT has a suppressive effect on the humoral and cellular components of an allergic reaction. After ASIT, the number of mast cells, neutrophils and eosinophils in the skin decreases, which leads to a decrease in the release of inflammatory mediators [5,6]. The most significant effect of ASIT is the formation of B cells synthesizing IgG4 and a gradual decrease in IgE titers, preventing a seasonal increase in IgE levels [2].

Changing the surface structure of antigens reduces the interaction with IgE, so such preparations can be used in doses significantly higher than the standard ones. One of the methods of surface modification is the encapsulation of the antigen in a polymer shell obtained on the basis of chitosan and its derivatives. Zheng-Shun Wen et al. [7] showed that chitosan nanoparticles can enhance cellular and humoral immune response and induce a balanced Th1/Th2 response. Additionally, a vaccine based on chitosan nanoparticles has been developed that significantly reduces inflammation of the respiratory tract in mice with bronchial asthma [8]. Krishnendu Roy et al. showed that oral immunization with nanoparticles synthesized by the complexation of peanut allergen DNA with chitosan was effective in reducing anaphylactic reactions in mice, which makes it possible to use such a vaccine for the treatment of food allergies [9]. None of these studies analyzed IgE production before and after ASIT.

In this work, core–shell Gal-MPs based on chitosan derivatives were developed for subcutaneous ASIT. The core contained recombinant Gal d1 protein immobilized on succinyl chitosan (SC) coated with the shell formed by quaternized chitosan (QC). Earlier, negatively charged core–shell chitosan-alginate nanoparticles of 500–700 nm in diameter able to prevent the allergen contact with mast cells, were developed [10]. However, negative charge and small size of the particles resulted in a relatively low IgG titers. In this work, positively charged Gal-MPs which effectively induced IgG response and blocked IgE were developed. The developed core–shell structure contributed to the rapid and safe production of IgG antibodies against allergens.

2. Materials and Methods

2.1. Materials

Crab chitosan with MW 200 kDa and a degree of deacetylation (DD) of 96% (Bioprogress, Moscow region, Russia), and N-[(2-hydroxy-3-trimethylammonium)propyl] chitosan chloride (QC) with MW 25 kDa and a degree of substitution (SD) of 98%, (a gift from Dr. B. Shagdarova, Laboratory of biopolymer Engineering of FITZ Biotechnology RAS, Moscow, Russia) were used. Chitosan derivatives were purified via reprecipitation and dialysis. Succinic acid anhydride (Honewell, Lincolnshire, IL, USA), 2-hydroxypropane-1,2,3-tricarboxylic acid, acetic acid, hydrochloric acid (HimMed, Moscow, Russia), N-(3-Dimethylaminopropyl)-N′-ethylcarbodiimide hydrochloride (EDAC), azacitidin, dimethyl sulfoxide (DMSO), paraformaldehyde (PFA), Hoechst 33342, 3,3′5,5′-tetramethylbenzidine (TMB) (Merck KGaA, Darmstadt, Germany), Alexa Fluor 488™ phalloidin (ThermoScientific, Wltham, MA, USA), Mowiol 4.88 (Calbiochem, Nottingham, UK), rodamine B-COOH (a gift of Dr. Yu. Gracheva, Nizhni Novgorod State University, Russia) were used. The remaining reagents had analytical purity and were used without additional purification.

2.2. Chitosan Succinylation

To obtain SC, 2 g of Chi with MW 25 kDa, DD 98%, obtained by acid hydrolysis of chitosan 200 kDa and CD 96% [11], was dissolved in 40 mL of 5% acetic acid followed by the addition of 160 mL of ethanol. The amount of succinic anhydride was calculated based on the ratio of v/v anhydride to amino groups (=20). Succinic anhydride was dissolved in a minimum volume of acetone and added to the Chi solution with stirring. The mixture was incubated overnight. The resulting gel was dissolved in distilled water and the pH was adjusted to 10 with 2 M NaOH. The resulting precipitate and solution were dialyzed against distilled water and lyophilized [12,13].

2.3. Physicochemical Characteristics of Chitosan Derivatives

The MW of chitosan derivatives were determined using high-performance gel-penetrating chromatography on the S 2100 Sykam chromatograph (Eresing, Germany) with a column (7.8 × 300 mm) Ultahydrogel-250 (Waters, Milford, MA, USA) and a pre-column (4 × 3 mm) GFC-4000 (Phenomenex, Torrance, CA, USA) [14].

The DD of chitosan samples and the SD of SC were determined using proton magnetic resonance (^{1}H-NMR). Proton spectra were recorded on a Bruker AMX 400 spectrometer (Camarillo, CA, USA). The samples were prepared in deuterated water, and 4,4-dimethyl-4-silapentane sulfonic acid was used as a standard.

2.4. Rhodamine Labeled Gal d1

Rodamine B-COOH (RhB-COOH), 0.8 mM in DMSO was mixed with 15 mM of EDAC in water, pH 6, and incubated for 20 min on ice with stirring. Gal d1, 5 mg, was dissolved in 200 µL of 0.05 M Na-bicarbonate buffer, pH 9.6 and mixed with the activated RhB-COOH. The reaction was carried out on ice overnight. The protein was then dialyzed three times against a phosphate-buffered solution (PBS) and freeze-dried.

2.5. Gel Electrophoresis

Gel electrophoresis was performed on 12% separating polyacrylamide gel and stained with Coomassie diamond blue R-250. The gels were documented on the Gel Doc EZ Imager device (BioRad Laboratories, Hercules, CA, USA).

2.6. Preparation of Core Particles using Citric Acid and EDAC

SC was dissolved in PBS, pH 7.2, at 2.5 mg/mL and left for 30 min with stirring to complete transparency. Then, 0.5 mg of Gal d1 or Gal-RhB was added. The ratio of antigen to SC was 1:5. Further, 0.6 mL of citric acid solution in water (4 mg/mL) with EDAC (8 mg/mL) was added drop by drop to the resulting solution with stirring to form core particles containing the conjugated allergen. The reaction mixture was stirred for 3 h at room temperature.

2.7. Preparation of Core Particles Using $CaCl_2$

SC was dissolved in PBS, pH 7.2, to a concentration of 2.5 mg/mL, and then Gal d1 was added at a ratio of 5:1. MPs were formed by the dropwise addition of 85 µL of 1% $CaCl_2$ solution was to 1 mL of the resulting solution. The reaction mixture was stirred for 3 h at room temperature.

2.8. Formation of Core–Shell Gal-MPs

Both types of core particles were coated with QC. To this end, 250 µL of QC solution per 1 mL of the core particles was added drop by drop by stirring for 30 min. During this time, a polyelectrolyte complex with a positive charge was formed. The resulting Gal-MPs were sterilized in a microwave oven (1 min in a water bath at maximum power). Sterility was confirmed in vitro.

2.9. Size and Charge of Gal-MPs

The size and charge of core and core–shell Gal-MPs was carried out via dynamic light scattering (DLS) using the 90 Plus Particle Size and ZetaPALS analyzer (Brookhaven, Vernon Hills, IL, USA) at a temperature of 25 °C, a fixed angle of 90° and a laser wavelength of 661 nm. The average values of the effective diameter and zeta potential were calculated from at least 5 independent measurements. The concentration of Gal d1 within the core and core–shell MPs was determined using spectrophotometer NanoDrop One (Thermo Scientific, Walthan, MA, USA).

2.10. Cell Cultures

Murine macrophage cells RAW264.7, fibroblasts L929, and human macrophage-like THP-1 cell line (IBCh collection, Moscow, Russia) were grown in RPMI-1640 supplemented with 10% fetal calf serum (FCS) and pen-strep-glut (complete culture medium) (all from PanEco, Moscow, Russian Federation) in CO_2 incubator at 37 °C. Cells were passaged twice a week using Trypsin/EDTA solution (PanEco, Moscow, Russia).

2.11. MTT-Assay

The cytotoxic effect of Gal-MPs was estimated using a standard 3-(4, 5-dimethyl-2-thiazolyl)-2, 5-diphenyl-2H-tetrazolium bromide (MTT, Sigma) assay. Briefly, different dilutions of Gal-MPs were prepared on a separate 96-well flat-bottom plate (Costar, Washington, WA, USA) and then transferred in 100 μL to the plates containing 5×10^3 cells/well. Non-treated cells served as controls. The plates were incubated for 72 h. For the last 3 h 10 μL of MTT (5 mg/mL) was added to each well. After the incubation, the culture medium was removed and 100 μL of DMSO was added to dissolve formazan crystals. Optical density was read on spectrophotometer Titertek (UK) at 540 nm. The results were analyzed using Excel package (Microsoft). The inhibition of proliferation (inhibition index, II) was calculated as $II = [1 - (OD_{experiment}/OD_{control})]$, where OD is the optical density. The experiments were repeated twice and average data are shown.

2.12. Bone Marrow Derived Macrophages and Dendritic Cells

BALB/c mice were euthanized by cervical dislocation. Bone marrow cells (BMCs) were obtained by flushing out femurs with PBS. Cells were cultured for 7 days at a density of $1.5–2 \times 10^6/cm^3$ in complete culture medium supplemented with 10% of L929 supernatant as a source of differentiation factors. All non-adhesive cells were discarded, adhesive cells were trypsinized, washed, and used for the analysis.

2.13. Confocal Microscopy

BMC macrophages, 10^5, were seeded onto sterile cover glasses (10^5/per well) and incubated in a CO_2 incubator at 37 °C until the cells adhered. Rh-labeled Gal-MPs were added and incubated for 18 h at 37 °C. At the end of the incubation, the cells were fixed with 1% PFA and washed three times with PBS 0.01% Triton X100. Fixed and permeabilized BMCs were stained with phalloidin AlexaFluor 488 (Applied Biosystems, Foster City, CA, USA) and nuclear dye Hoechst 33342 (Merck KGaA, Darmstadt, Germany) for 1 h. Cells were polymerized with Mowiol (Calbiochem, Nottingham, UK) and analyzed using a TE 2000 Eclipse confocal microscope (Nikon, Tokyo, Japan).

2.14. Flow Cytometry

To analyze cytotoxicity and Gal–MPs interaction with the antigen presenting cells via flow cytometry, human macrophage-like THP-1 cell line was used. Gal-Rh-MPs were incubated with 10^6 cells/well for 18 h and stained with 50 μg/mL of propidium iodide (Sigma, Merck KGaA, Darmstadt, Germany), incubated for 15 min, and analyzed. The analysis was carried out using FACScan flow cytometer (BD, Franklin Lakes, NJ, USA). Calculation of the results was carried out using the program FlowJo (USA). BMC macrophages were

characterized by the expression of CD11b and CD11c markers using specific antibodies (Biolegend, San Diego, CA, USA).

2.15. Mice

Female BALB/c mice (25 ± 5 g) were obtained from the laboratory animal nursery "Pushchino", Moscow region. The mice were housed in plastic cages, 10–12 mice per cage, under conventional minimal pathogen conditions. They were kept in a 12 h light/dark cycle at room temperature and fed ad libitum. Mice were euthanized by cervical dislocation. The research protocol was approved by the Ethical Committee of the Institute of Bioorganic Chemistry of the Russian Academy of Sciences, Protocols No. 232 (2018) and No. 327 (2021).

2.16. ASIT

Mice (n = 30) were divided into 6 groups and were injected subcutaneously in a foot pad 6 times with 2–3 day intervals: intact mice (n = 5) were injected with PBS; mice from group 1 (n = 5) were injected with Gal-d1; mice from group 2 (n = 5) were injected with Gal-SC 1; mice from group 3 (n = 5) were injected with Gal-MPs 1; mice from group 4 (n = 5) were injected with Gal-SC 2; and mice from group 5 (n = 5) were injected with Gal-MPs 2. The injection contained 30 μg of Gal d1. Blood was collected from the orbital sinus using isofluran anesthesia before and after immunization. Serum was collected and stored at −20 °C before use.

2.17. Allergy Model

A low-dose allergy model was used to induce IgE to Gal d1 [10]. Briefly, mice (n = 5) were injected into the withers 9 times with 100 ng/mouse of Gal d1 in saline. To estimate the ASIT effect, a group of mice (n = 5) was previously vaccinated with Gal-MPs 1, as described above. One month after vaccination, mice were treated to induce allergic IgE response. To estimate the safety of ASIT, mice with Gal d1-induced IgE were injected with Gal-MPs. Local reaction was analyzed based on body temperature and skin rash reaction.

2.18. Enzyme Immunoassay (ELISA)

ELISA was performed on 96-well microtitration plates (Costar, Washington, WA, USA) coated with 5 μg/mL of Gal d1 or Gal-MPs in 0.05 M Na-bicarbonate buffer, with pH 9.6. The plates were incubated overnight at +4 °C. The plates were washed between each incubations with PBS 0.05% Tween-20 (PBS-T). All incubations with serum and specific antibodies were conducted in PBS-T with 5% non-fat dry milk at room temperature for 1 h. Anti-mouse IgG-HRP or IgE-HRP (Abcam, Cambridge, UK) levels were estimated using TMB substrate. The optical density was measured using a spectrophotometer (Thermo Fisher Scientific, Waltham, MA, USA) at 450 nm with subtraction of the optical density at 620 nm. The number of antibodies was evaluated as titers corresponding to the maximum serum dilutions, at which the optical density (OD) was 3 SD deviations higher than the average background.

2.19. Histology

Withers tissue samples were fixed in 4% paraformaldehyde and embedded in paraffin. Samples were cut into sections with a thickness of 4 μm using Leica RM 2145 RTS microtome (Leica Biosystems, Amsterdam, The Netherlands). After dewaxing of tissue sections, they were stained with H&E according to the manufacturer's protocols. Then, the sections were dehydrated, clarified, and enclosed under a cover glass using the Consul-Mount histological medium.

2.20. Statistical Analysis

Graphs were created using MS Excel software. The data are represented as mean ± SD of at least two independent experiments or as one representative experiment. The

parametric *t*-test was used to compare the experimental groups. Levels of $p < 0.05$ were considered statistically significant.

3. Results

3.1. Characterization of Chitosan Derivatives and Core–Shell Particles

Chitosan with MW 25 kDa was obtained via acidic hydrolysis of the MW 200 kDa sample (Figure 1a). Chitosan 25 kDa was modified with succinic acid residues in order to obtain negatively charged derivative SC with increased solubility at neutral pH. The ^{1}H-NMR spectrum showed that substitution degree of SC was 43% (Figure 1b).

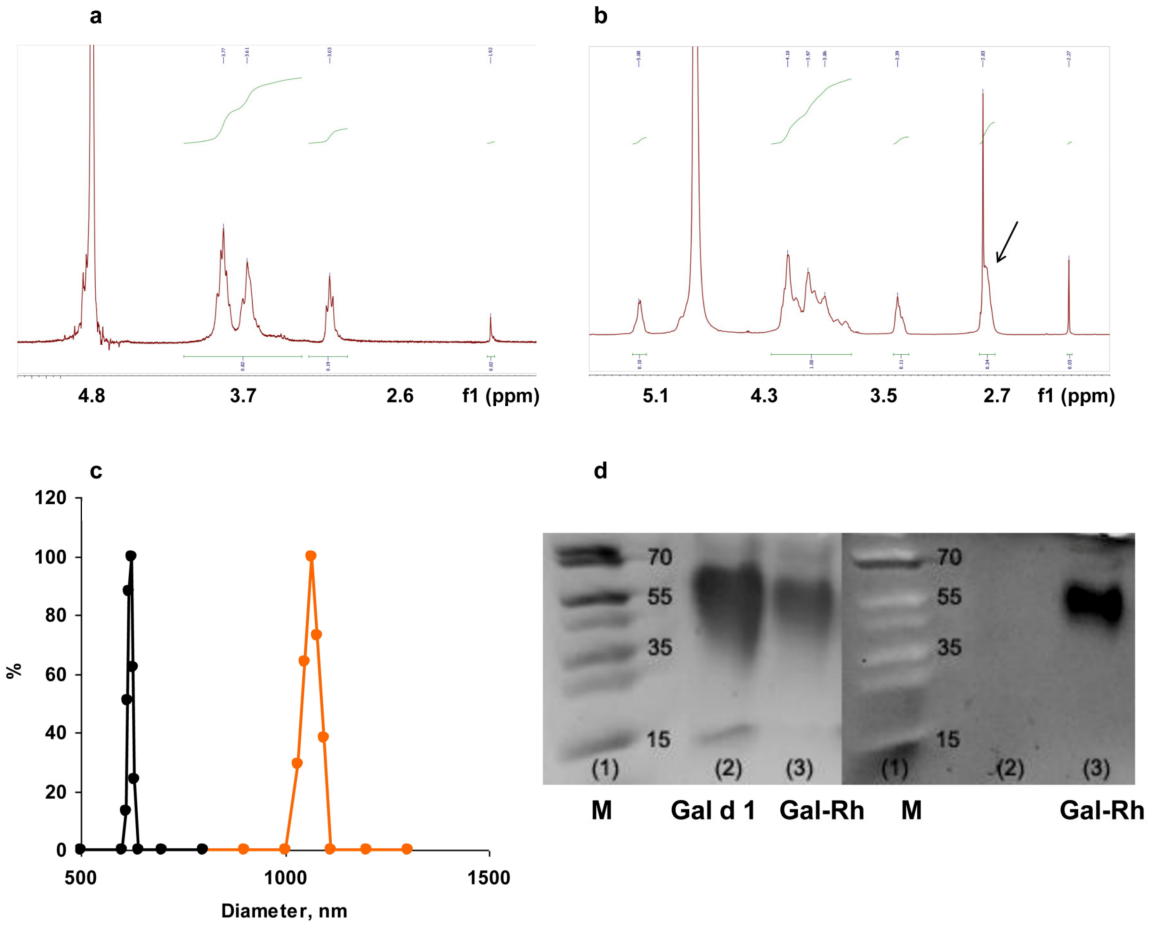

Figure 1. Characterization of chitosan derivatives and Gal-MPs: (**a**) ^{1}H-NMR spectra of chitosan MW 25 kDa and DD 98% and (**b**) succinyl chitosan MW 25 kDa and SD 43% (arrow). (**c**): DLS of core particles (black line) and core–shell particles containing Gal d1 allergen. (**d**): Gel electrophoresis of Gal d1 and Gal d1-Rh in white light (left) and UV (right). M—MW ladder.

Core particles, containing the model allergen Gal d1, were prepared using two methods: EDAC/citric acid and $CaCl_2$ precipitation. Both methods produced microparticles Gal-MPs of 600–700 nm in diameter (Figure 1c, black line). Coating with QC resulted in 1100–1300 nm particles (Figure 1c, orange line). There were no statistical differences in the diameter between Gal-MPs obtained via EDAC/citric acid or $CaCl_2$ precipitation. Core Gal-SC particles were negatively charged ($\zeta = -10$–11 mV) while coating with QC resulted in positively charged Gal-MPs ($\zeta = +9$ mV). Positive charge of MPs should potentially increase an interaction with negatively charged antigen presenting cells. The protein concentration in Gal-MPs was around 300–400 µg/mL. The characteristics of the Gal-MPs obtained using the two different methods are shown in Table 1.

Table 1. Parameters of Gal-MPs obtained using the two methods.

	Diameter, nm	ζ Potential, mV	Gal d1 Concentration, μg/mL
	EDAC/citric acid		
Core, Gal-SC 1	710 ± 12	−11 ± 2	350 ± 50
Core–shell, Gal-MPs 1	1230 ± 44	+9 ± 5	350 ± 65
$CaCl_2$ precipitation			
Core, Gal-SC 2	680 ± 15	−10 ± 3	340 ± 35
Core–shell, Gal-MPs 2	1180 ± 53	+9 ± 5	340 ± 55

To visualize the Gal-MPs, Gal d1 was labeled with rhodamine B. The conjugation slightly increased the MW of Gal d1 (Figure 1d, left panel). Documentation of this gel in UV showed a bright fluorescence of Gal-Rh-MPs (Figure 1d, right panel).

3.2. Cytotoxicity of Gal-MPs

The cytotoxicity of Gal-SC core particles and Gal-MPs was studied in a mouse macrophage cell line RAW 264.7, mouse fibroblast-like cell line L929, and human macrophage-like THP-1 cell line. The results demonstrated low toxicity at 5% of core Gal-SC and core–shell Gal-MPs and stimulation of the cell proliferation at the dilutions more than 100 times (Figure 2a,b). No difference was found between core and core–shell activity.

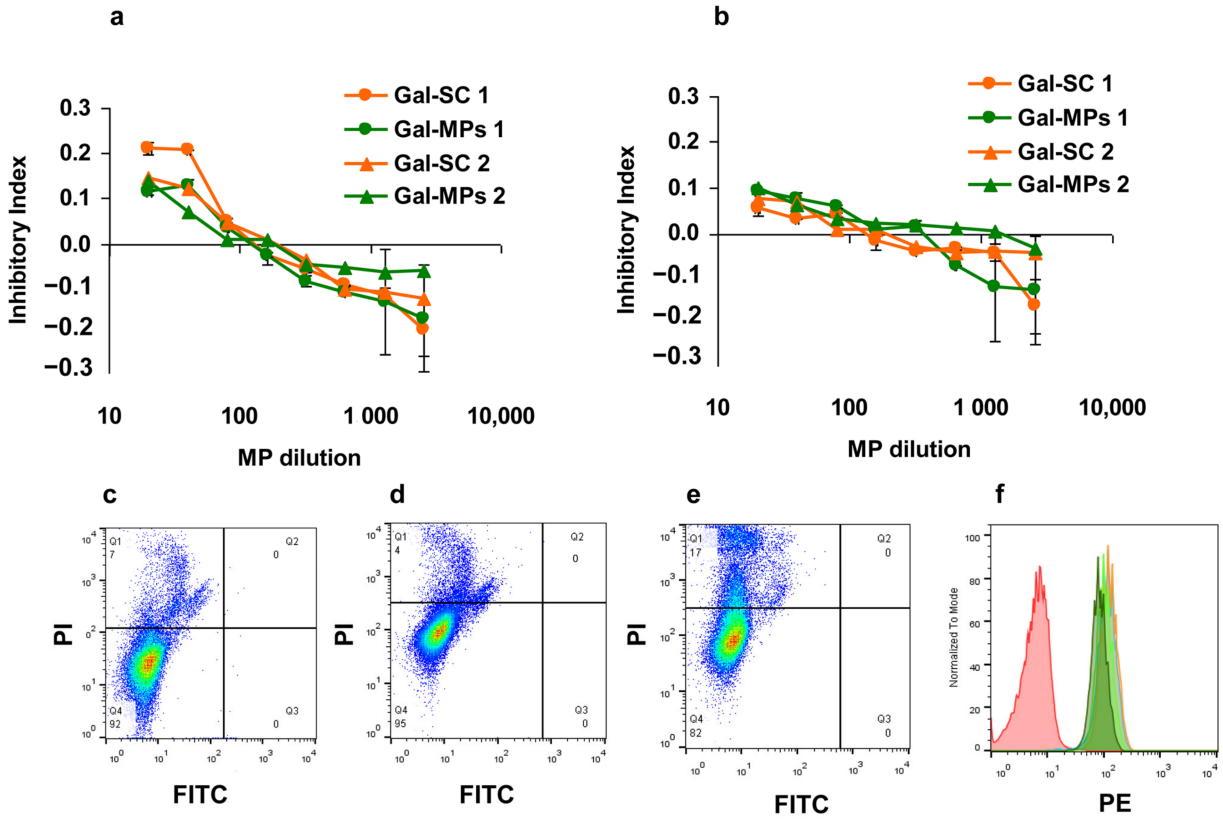

Figure 2. Cytotoxicity of Gal-MPs. (**a**,**b**): Inhibition of RAW264.7 (**a**) and L929 (**b**) cell proliferation by core Gal-SC and core–shell Gal-MPs, where 1 and 2 correspond to two methods of core preparation (Table 1). (**c**–**e**): Analysis of the percentages of dead cell estimated using propidium iodide (ordinate) in control THP-1 cells (**c**) and after incubation for 18 h with Gal-SC1 (**d**) or Gal-MPs 1 (**e**). (**f**): Binding of Gal-Rh-SC and Gal-Rh-MPs (right overlaid peaks) and control fluorescence (left pink peak).

To analyze cytotoxicity and Gal–MPs interaction with the antigen presenting cells via flow cytometry, human macrophage-like THP-1 cell line was used. This cell line is

nonadhesive which makes it easy to be treated and be analyzed using the flow method. To conduct the test, fluorescently labelled Gal-Rh-MPs were incubated with THP-1 cells for 18 h and analyzed. Cytotoxicity of the preparations was analyzed using propidium iodide (PI) cell staining. The results showed that core–shell Gal-MPs, but not core Gal-SCs, were toxic at the concentration used. Cytotoxicity of the core Gal-SC particles did not differ from the control cells and the percentage of dead cells was 7 and 5% accordingly (Figure 2c,d), while quaternized positively charged Gal-MPs were more toxic; and the percentage of PI+ cells was 17–20% (Figure 2e). Earlier, it has been shown that highly quaternized (i.e., high ζ-potential) chitosan indeed was toxic to the cells while negatively charged chitosan derivatives were non-toxic [15].

Analysis of Gal-MPs binding to THP-1 cells demonstrated that up to 100% of cells were positive (Figure 2f).

3.3. Binding of Gal-MPs to Bone Marrow Dendritic Cells

The membranes of mammalian cells are negatively charged. Positively charged Gal-MPs primarily interact with the cells due to electrostatic interactions. To visualize cell–particle interactions with the antigen-presenting cells, dendritic cells from murine bone marrow were generated. The bone marrow cells were incubated with supernatant from the L929 cells for 7 days. Adhesive cells were collected and analyzed using flow cytometry. The results demonstrated that all cells were CD11b and CD11c positive, which is specific for dendritic cells (data not shown). Dendritic cells were incubated during 1, 6 or 18 h with Gal-MPs. Already, 1 h incubation resulted in some binding of Gal-MPs to the cells (Figure 3a, thin white arrows) with multiple particles present around the cells; 6 h later some Gal-MPs were found inside some cells (Figure 3b); and at 18 h multiple Gal-MPs were found inside the cells (Figure 3c, thick arrows). Phagocytosis induced the formation of pseudopods in the dendritic cells (Figure 3, arrow heads). Incubation of the cells with the core particles also resulted in the internalization (Figure 3d), however, their numbers inside the cells were lower in comparison with Gal-MPs. Higher magnification showed that Gal-MPs were round with an empty core and non-smooth surface (Figure 3e). As soon as rhodamine was bound only to Gal d1, we hypothesized that the protein was exposed on the SC core surface and covered by QC (Figure 3f).

3.4. IgE Reactivity of Gal-MPs

Vaccines for ASIT must be safe. The first problem during ASIT is the activation and degranulation of the resident mast cells harboring IgE from blood via the high affinity IgE receptor (FcεRI). This reaction is induced when allergen comes into contact with IgE bound to FcεRI on mast cells. Multiple binding of an allergen is required for mast cell degranulation. Consequently, Gal d1 encapsulated into Gal-MPs must not bind to specific IgE. To this end, Gal d1, core Gal-SC and core–shell Gal-MPs were used as coating antigens in the ELISA. IgE specific to Gal d1 sera were used to estimate binding to the encapsulated Gal d1. The results demonstrated a complete protection of the encapsulated Gal d1 from IgE binding (Figure 4a). Even core Gal-SC particles were effective in the protection of the allergen from IgE contact.

3.5. Immunogenicity of the Encapsulated Gal d1

Encapsulated proteins must retain their immunogenicity. Mice were immunized with 30 μg/ per injection of Gal-MPs in 50 μL of saline. Mice were injected subcutaneously in the paw pad six times for an interval of 2–3 days (Figure 4b, red arrow). Blood was collected two weeks post vaccination and analyzed for Gal d1-specific IgG and IgE production. Immunization with Gal d1 in saline resulted in low IgG production. Both types of core Gal-SC particles increased IgG titers by 200 times higher and both core–shell Gal-MPs increased it 560 times higher than free Gal d1 (Figure 4c,d). No IgE production was induced by the encapsulated Gal d1.

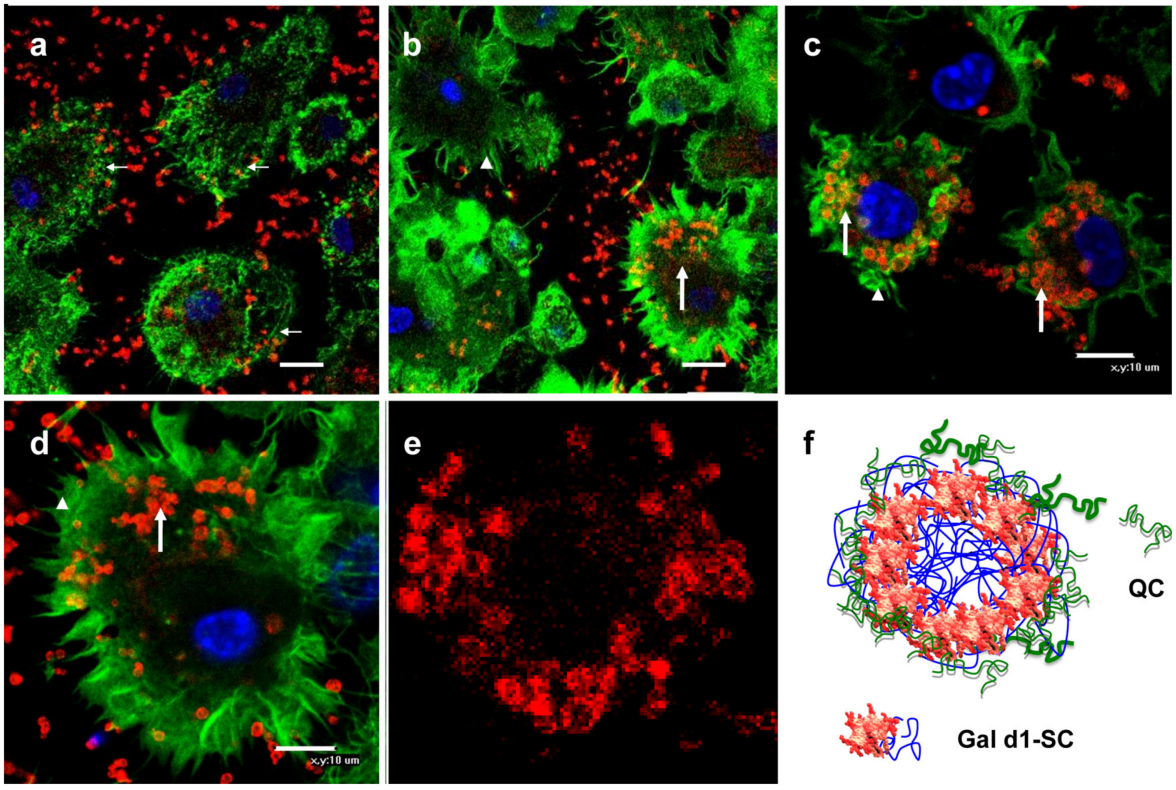

Figure 3. Binding of Gal-MPs by dendritic cells. (**a**–**c**): Differentiated bone marrow dendritic cells were incubated with Gal-MPs (red) for 1 (**a**), 6 (**b**) or 18 (**c**) h. Arrows show intracellular location of the NPs, arrow heads show relocation of F-actin (green). (**d**): Binding of core Gal-SC1. (**e**): Overview of Gal-MPs within the cells. BM cells are stained in F-actin (green) and nuclei (blue). Scale bar 10 µm. (**f**): Hypothetical structure of Gal-MPs where Gal d1 is shown in red, succinyl chitosan (SC)—in blue, quaternized chitosan (QC)—in green color.

These results show that the encapsulated allergens (i) do not bind IgE; (ii) induce allergen specific IgG production at high titers in a short time; and (iii) that core–shell particles are more efficient in IgG induction compared to the core ones either due to the positive charge or the larger diameter.

3.6. Can Subcutaneous ASIT with the Encapsulated Allergens Protect from Allergy?

The final question in this study was to determine whether IgG of Gal d1 induced by the vaccination of mice with the encapsulated allergen prevents or at least decreases IgE formation when the allergen interacts with the immune cells via mucosal barriers. Earlier, the low-dose allergy model where mice were sensitized with low doses of allergens, such as 100 ng/injection, 9–10 injections into the withers of mice, has been developed by us. Such protocol results in high IgE and relatively low IgG production [16]. This model was used to induce IgE to Gal d1 in the mice vaccinated with Gal-MPs (Figure 5a). Intact mice were sensitized with Gal d1 as a control with an allergic response to Gal d1. In clinical practice, ASIT does not prevent IgE synthesis, however, it alleviates symptoms [17]. Our results showed a complete prevention of the IgE increase induced by the allergen injections (Figure 5b). Histological analysis of the withers demonstrated a higher vascularization in the vaccinated mice (Figure 5(c2), red arrows) in comparison with intact withers (Figure 5(c1)). Allergy formation was associated with the formation of immune clusters where B-cells can be switched to IgE (Figure 5(c3), black arrows). No immune clusters were found in the withers of the vaccinated mice (Figure 5(c2)). The Gal d1 injection in allergic mice also induce IgG production (Figure 5d).

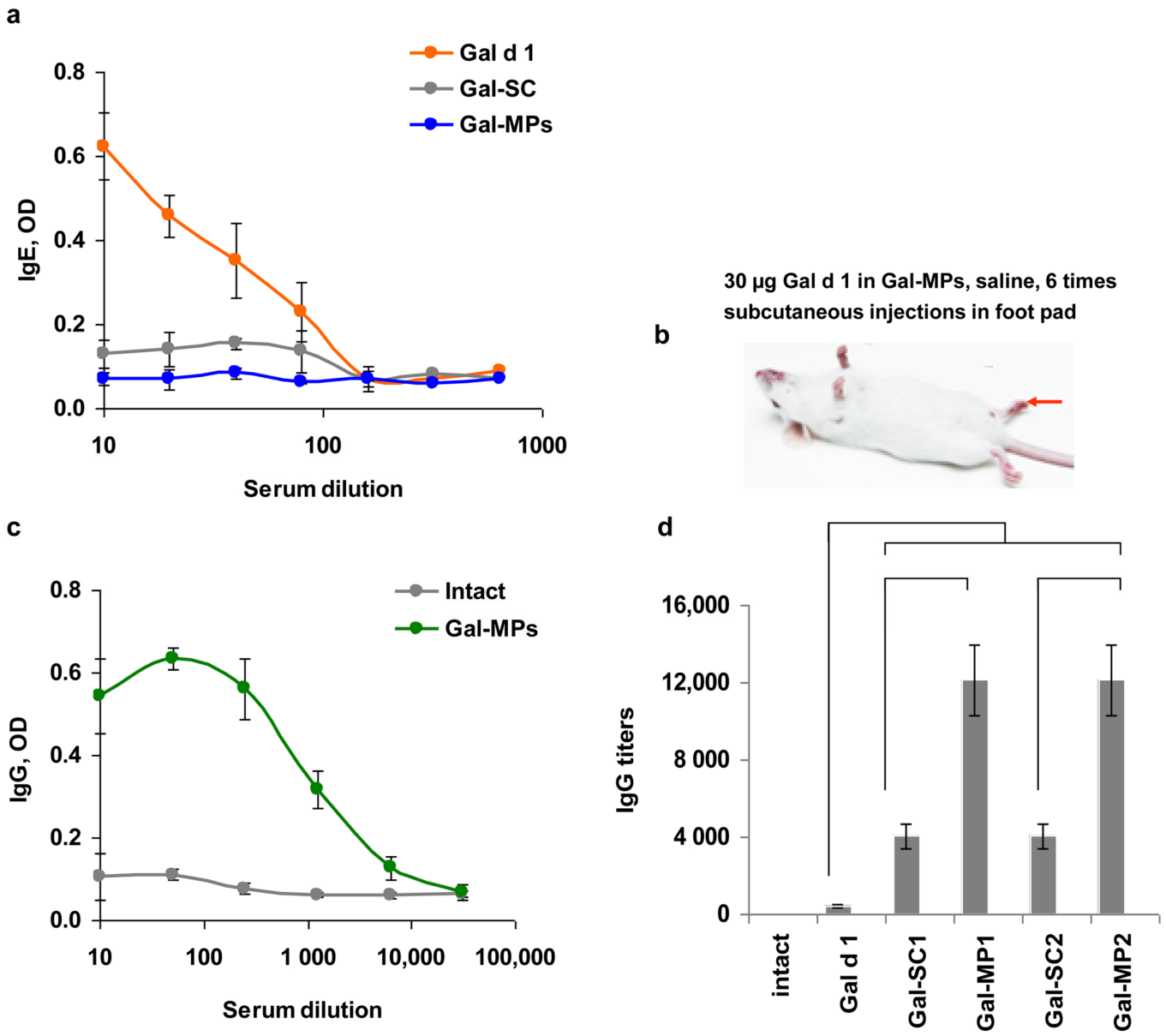

Figure 4. IgE reactivity and immunogenicity of the encapsulated Gal d1. (**a**): Gal d1-specific IgE binding to Gal d1, Gal-SC or Gal-MPs. (**b**): BALB/c mice were immunized s.c. in the paw pad (red arrow) with 30 µg of the encapsulated Gal-MPs 6 times with an interval of 2–3 days. (**c**,**d**): Titration curves (**c**) and IgG titers (**d**) in the blood of mice immunized with Gal d1, Gal-SC1, Gal-MPs1, Gal-SC2, Gal-MPs2. Statistical difference ($p < 0.01$, *t*-test) is shown with brackets.

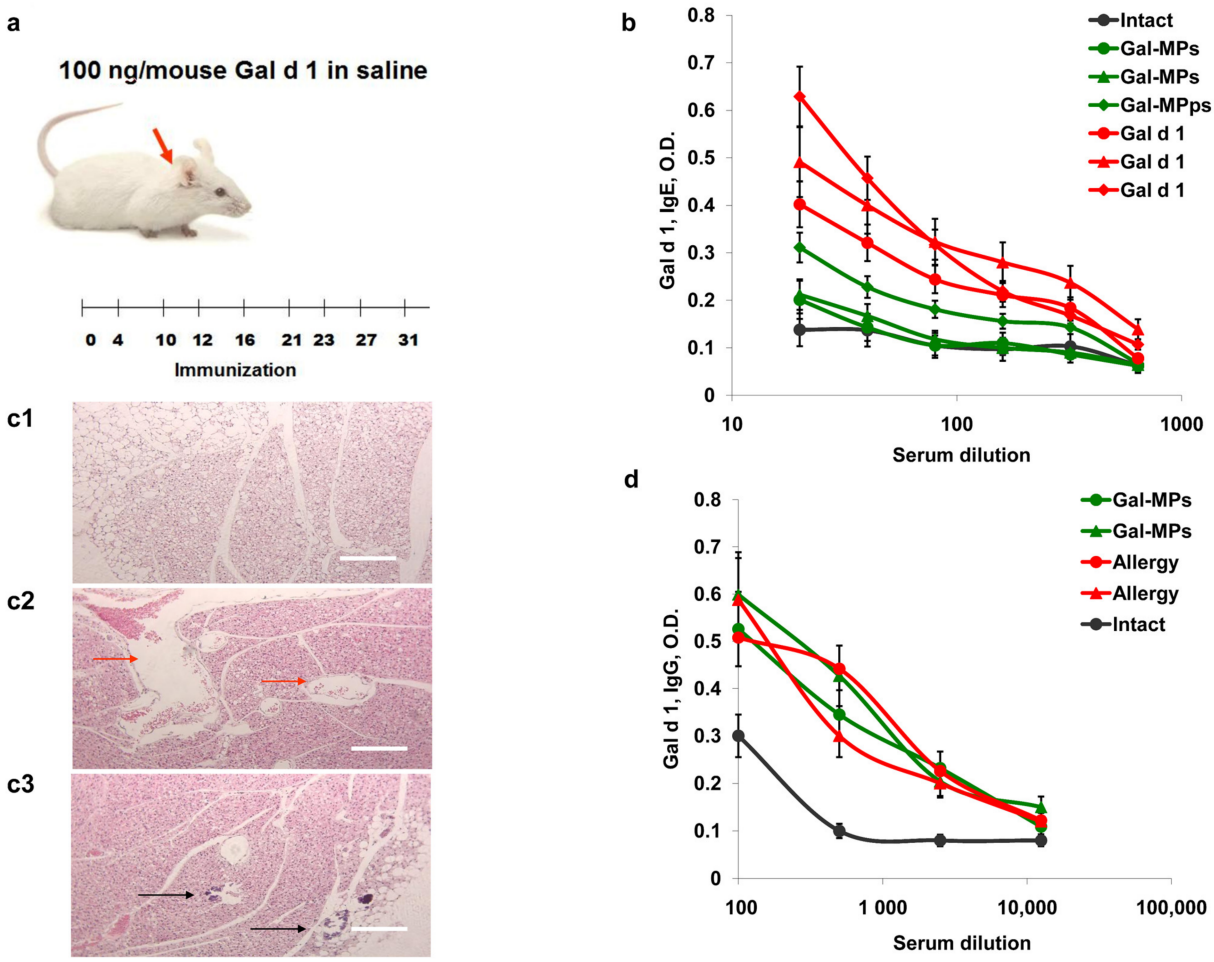

Figure 5. Allergic response in the Gal-MP vaccinated mice. (**a**): BALB/c mice intact and vaccinated were injected into the withers (red arrow) with 100 ng/injection Gal d1 in saline 9 times with 2–3 day intervals. (**b**–**d**): Gal d1 specific IgE (**b**) and IgG (**d**) levels in the blood of intact, vaccinated, and allergic mice (individual mice). (**c**): Histology of the withers of intact (**c1**), vaccinated (**c2**), and allergic unvaccinated (**c3**) mice. The red arrows shown a higher vascularization in the vaccinated mice (**c2**); black arrows shown the formation of immune clusters where B-cells can be switched to IgE (**c3**). H&E. Scale bars 100 μm.

4. Discussion

Chitosan is an aminopolysaccharide obtained from chitin via N-deacetylation. It has free amino groups (-NH_2), which opens up wide possibilities for chitosan modification. SC derivatives are obtained via acylation with succinic anhydride in an organo-aqueous medium, containing1% acetic acid and acetone, to dissolve the anhydride. The reaction proceeds with the opening of the anhydride ring. The SD of an acyl residue depends on the ratio of reagents in the reaction [18]. SC is used in various drug delivery systems to deliver insulin, anticancer agents, genetic material [19–21], etc. Methods to obtain chitosan-based nanoparticles include ionic gelation, emulsion, reverse micellar method, coacervation, deposition, nanoprecipitation, and sieving method [22]. Chitosan-based nanoparticles are good carriers due to properties, such as hydrophilicity, non-toxicity, biodegradability, biocompatibility and bioadhesiveness [23]. In this work, the allergen Gal d1 ovomucoid with MW 28 kDa, which is a major hen egg's allergen [24], was used to be encapsulated into MPs. Core Gal-SCs were obtained using either a crosslinking agent citric acid activated using carbodiimide or $CaCl_2$ precipitation. As the results of the confocal microscopy showed, Gal d1 was found on the surface of SC particles. This packaging may not completely cover some epitopes on the surface of the particles sufficient for their

recognition by IgE. Therefore, the next step was to cover Gal d1 by the shell. To develop the shell, we used positively charged chitosan derivative QC with a high SD. SC and QC formed a polyelectrolyte complex due to electrostatic interactions.

Biomedical applications of any preparation requires high safety requirements. Previously, it has been shown that the toxicity of chitosan and its derivatives is determined mostly by their charge. Regardless of the degree of acetylation, molecular weight, and hydrophobicity, only highly positively charged chitosan derivatives, namely quaternized one with SD more than 80%, at high concentration inhibited the proliferation of cells [25]. Multiple studies show that chitosan-based materials mainly are low toxic to cells [26,27]. However, some toxicity of positively charged MPs can serve as an additional adjuvant for the tissue resident antigen-presenting cells [28]. Multiple studies have shown that chitosan-based delivery systems stimulate antibody production, cytokine synthesis, and functional effects of proteins, peptides, and DNA encapsulated into nano- and microparticles [7–9,28]. Our results supported these findings and showed the induction of IgG response to Gal d1 in mice immunized by six injections of Gal-MPs. Gal-SC particles were less effective in IgG induction in a comparison with core–shell Gal-MPs. This can be a result of the positive charge of Gal-MPs, however, the size of the particles also can play a role.

The specific characteristic of Gal-MPs was their bi-layer structure designed to cover possible allergen IgE binding sites. Analysis of IgE binding showed that even core Gal-SC particles did not bind IgE, however, we think that for a better safety core–shell particles are preferable.

The size of the delivery system depends on the planned application. The delivery vehicle must be small (50–150 nm) for the intravenous injections or tissue injections, such as the eye, where the cargo must be released within a prolonged time [29]. Contrary to it, vaccines are designed to be quickly engulfed by the resident tissue macrophages and dendritic cells. Evolutionally macrophages better phagocyte large objects while dendritic cells are able to uptake soluble antigens by endocytosis. We showed that larger Gal-MPs were better delivered to the antigen presenting cells than Gal-SC, resulting in a lower IgG production.

The last part of our work was devoted to the verification that the vaccination with the encapsulated allergens can modify allergic response. It has been shown that the preventive vaccination with Gal-MPs can abrogate IgE formation to Gal d1.

5. Conclusions

The aim of this work was to develop a new pathway to prevent the formation of IgE-mediated allergy. We showed that an allergen encapsulated into core–shell chitosan microparticles induced a high IgG response which protected mice from IgE formation. Different suitable methods can be applied to develop delivery systems based on chitosan derivatives. There was no difference in the functional activity of the particles sensitized using different methods. In our opinion, positively charged microparticles are preferable for ASIT vaccines. Their diameter can be up to 2–3 μm, which is the size of the bacteria. Hypothetically ASIT can be conducted in predisposed persons. In this case, a complete protection can be achieved. However, further research will show whether such vaccines can reduce IgE production in allergic persons. One more possibility, which also requires additional study, is the production of polyvalent vaccines containing several major allergens from the natural source.

Author Contributions: Conceptualization, E.S. and E.K.; methodology, E.K.; nanoparticles obtaining and analysis K.B., O.K., G.F. and M.K.; biological investigation, K.B., O.K., G.F. and M.K.; validation, formal analysis and data curation, E.S., M.K. and G.F.; writing—original draft preparation, E.K., M.K. and E.S.; writing—review and editing, E.S., G.F. and E.K.; visualization, M.K. and E.S.; supervision, E.S.; project administration, E.S. and E.K.; funding acquisition, E.K. All authors have read and agreed to the published version of the manuscript.

Funding: This research was funded by the Russian Foundation for Basic Research, grant number 20-015-00360.

Institutional Review Board Statement: The animal study protocol was approved by the Ethics Committee of the Shemyakin & Ovchinnikov Institute of Bioorganic Chemistry of the Russian Academy of Sciences, protocols #232 (2018) and #327 (2021).

Informed Consent Statement: Not applicable.

Data Availability Statement: The data that support the findings of this study are available on request from the corresponding author.

Acknowledgments: We are thankful to B. Shagdarova for the quaternized chitosan (Biopolymer Engineering Laboratory of the FITZ Biotechnology RAS, Moscow) and A. Dolgova (St. Petersburg Pasteur Institute of Epidemiology and Microbiology, Saint Petersburg, Russia) for providing us with the recombinant Gal d1.

Conflicts of Interest: The authors declare no conflict of interest.

References

1. Jacobsen, L.; Wahn, U.; Bilo, M.B. Allergen-Specific Immunotherapy Provides Immediate, Long-Term and Preventive Clinical Effects in Children and Adults: The Effects of Immunotherapy Can Be Categorised by Level of Benefit—The Centenary of Allergen Specific Subcutaneous Immunotherapy. *Clin. Transl. Allergy* **2012**, *2*, 8. [CrossRef] [PubMed]
2. Ravetch, J.V. Fc Receptors. *Curr. Opin. Immunol.* **1997**, *9*, 121–125. [CrossRef] [PubMed]
3. Cooper, P.J. Interactions between Helminth Parasites and Allergy. *Curr. Opin. Allergy Clin. Immunol.* **2009**, *9*, 29. [CrossRef] [PubMed]
4. Akdis, C.A.; Akdis, M. Mechanisms of Allergen-Specific Immunotherapy and Immune Tolerance to Allergens. *World Allergy Organ. J.* **2015**, *8*, 17. [CrossRef] [PubMed]
5. Jutel, M.; Akdis, M.; Budak, F.; Aebischer-Casaulta, C.; Wrzyszcz, M.; Blaser, K.; Akdis, C.A. IL-10 and TGF-β Cooperate in the Regulatory T Cell Response to Mucosal Allergens in Normal Immunity and Specific Immunotherapy. *Eur. J. Immunol.* **2003**, *33*, 1205–1214. [CrossRef]
6. Verhoef, A.; Alexander, C.; Kay, A.B.; Larché, M. T Cell Epitope Immunotherapy Induces a CD4+ T Cell Population with Regulatory Activity. *PLoS Med.* **2005**, *2*, 0253–0261. [CrossRef]
7. Wen, Z.-S.; Xu, Y.-L.; Zou, X.-T.; Xu, Z.-R. Chitosan Nanoparticles Act as an Adjuvant to Promote Both Th1 and Th2 Immune Responses Induced by Ovalbumin in Mice. *Mar. Drugs* **2011**, *9*, 1038–1055. [CrossRef]
8. Yang, W.; Dong, Z.; Li, Y.; Zhang, Y.; Fu, H.; Xie, Y. Therapeutic Efficacy of Chitosan Nanoparticles Loaded with BCG-Polysaccharide Nucleic Acid and Ovalbumin on Airway Inflammation in Asthmatic Mice. *Eur. J. Clin. Microbiol. Infect. Dis.* **2021**, *40*, 1. [CrossRef]
9. Roy, K.; Mao, H.Q.; Huang, S.K.; Leong, K.W. Oral Gene Delivery with chitosan–DNA Nanoparticles Generates Immunologic Protection in a Murine Model of Peanut Allergy. *Nat. Med.* **1999**, *5*, 387–391. [CrossRef]
10. Kashirina, E.; Reshetov, P.; Alekseeva, L.; Berzhets, V.; Ryazantsev, D.; Zubov, V.; Chudakov, D.; Svirshchevskaya, E. Encapsulation of Allergens into Chitosan-Alginate Nanoparticles Prevents IgE Binding. *Jacobs J. Vaccines Vaccin.* **2015**, *1*, 12.
11. Konovalova, M.V.; Kurek, D.V.; Litvinets, S.G.; Martinson, E.A.; Varlamov, V.P. Preparation and Characterization of Cryogels Based on Pectin and Chitosan. *Prog. Chem. Appl. Chitin Its Deriv.* **2016**, *21*, 114–121. [CrossRef]
12. Konovalova, M.; Shagdarova, B.T.; Zubov, V.; Svirshchevskaya, E. Express Analysis of Chitosan and Its Derivatives by Gel Electrophoresis. *Prog. Chem. Appl. Chitin Its Deriv.* **2019**, *XXIV*, 84–95. [CrossRef]
13. Yamaguchi, R.; Arai, Y.; Itoh, T.; Hirano, S. Preparation of Partially N-Succinylated Chitosans and Their Cross-Linked Gels. *Carbohydr. Res.* **1981**, *88*, 172–175. [CrossRef]
14. Lopatin, S.A.; Derbeneva, M.S.; Kulikov, S.N.; Varlamov, V.P.; Shpigun, O.A. Fractionation of Chitosan by Ultrafiltration. *J. Anal. Chem.* **2009**, *64*, 648–651. [CrossRef]
15. Zubareva, A.; Shagdarova, B.; Varlamov, V.; Kashirina, E.; Svirshchevskaya, E. Penetration and Toxicity of Chitosan and Its Derivatives. *Eur. Polym. J.* **2017**, *93*, 743–749. [CrossRef]
16. Chudakov, D.B.; Ryasantsev, D.Y.; Tsaregorotseva, D.S.; Kotsareva, O.D.; Fattakhova, G.V.; Svirshchevskaya, E.V. Tertiary Lymphoid Structure Related B-Cell IgE Isotype Switching and Secondary Lymphoid Organ Linked IgE Production in Mouse Allergy Model. *BMC Immunol.* **2020**, *21*, 45. [CrossRef]
17. Durham, S.R.; Shamji, M.H. Allergen Immunotherapy: Past, Present and Future. *Nat. Rev. Immunol.* **2023**, *23*, 317–328. [CrossRef]
18. Carreño-Gómez, B.; Duncan, R. Evaluation Of the Biological Properties of Soluble Chitosan and Chitosan Microspheres. *Int. J. Pharm.* **1997**, *148*, 231–240. [CrossRef]
19. Mukhopadhyay, P.; Sarkar, K.; Bhattacharya, S.; Bhattacharyya, A.; Mishra, R.; Kundu, P.P. pH Sensitive N-Succinyl Chitosan Grafted Polyacrylamide Hydrogel for Oral Insulin Delivery. *Carbohydr. Polym.* **2014**, *112*, 627–637. [CrossRef]

20. Yan, C.; Chen, D.; Gu, J.; Qin, J. Nanoparticles of 5-Fluorouracil (5-FU) Loaded N-Succinyl-Chitosan (Suc-Chi) for Cancer Chemotherapy: Preparation, Characterization—In-Vitro Drug Release and Anti-Tumour Activity. *J. Pharm. Pharmacol.* **2010**, *58*, 1177–1181. [CrossRef]
21. Toh, E.K.W.; Chen, H.Y.; Lo, Y.L.; Huang, S.J.; Wang, L.F. Succinated Chitosan as a Gene Carrier for Improved Chitosan Solubility and Gene Transfection. *Nanomed. Nanotechnol. Biol. Med.* **2011**, *7*, 174–183. [CrossRef] [PubMed]
22. Mohammed, M.A.; Syeda, J.T.M.; Wasan, K.M.; Wasan, E.K. An Overview of Chitosan Nanoparticles and Its Application in Non-Parenteral Drug Delivery. *Pharmaceutics* **2017**, *9*, 53. [CrossRef] [PubMed]
23. Iacob, A.T.; Lupascu, F.G.; Apotrosoaei, M.; Vasincu, I.M.; Tauser, R.G.; Lupascu, D.; Giusca, S.E.; Caruntu, I.D.; Profire, L. Recent Biomedical Approaches for Chitosan Based Materials as Drug Delivery Nanocarriers. *Pharmaceutics* **2021**, *13*, 587. [CrossRef] [PubMed]
24. Urisu, A.; Kondo, Y.; Tsuge, I. Hen's Egg Allergy. *Chem. Immunol. Allergy* **2015**, *101*, 124–130. [CrossRef] [PubMed]
25. Svirshchevskaya, E.V.; Zubareva, A.A.; Boyko, A.A.; Shustova, O.A.; Grechikhina, M.V.; Shagdarova, B.T.; Varlamov, V.P. Analysis of Toxicity and Biocompatibility of Chitosan Derivatives with Different Physico-Chemical Properties. *Appl. Biochem. Microbiol.* **2016**, *52*, 483–490. [CrossRef]
26. Chollakup, R.; Uttayarat, P.; Chworos, A.; Smitthipong, W. Noncovalent Sericin-Chitosan Scaffold: Physical Properties and Low Cytotoxicity Effect. *Int. J. Mol. Sci.* **2020**, *21*, 775. [CrossRef]
27. Li, D.; Liu, P.; Hao, F.; Lv, Y.; Xiong, W.; Yan, C.; Wu, Y.; Luo, H. Preparation and Application of Silver/chitosan-Sepiolite Materials with Antimicrobial Activities and Low Cytotoxicity. *Int. J. Biol. Macromol.* **2022**, *210*, 337–349. [CrossRef]
28. Walter, F.; Winter, E.; Rahn, S.; Heidland, J.; Meier, S.; Struzek, A.M.; Lettau, M.; Philipp, L.M.; Beckinger, S.; Otto, L.; et al. Chitosan Nanoparticles as Antigen Vehicles to Induce Effective Tumor Specific T Cell Responses. *PLoS ONE* **2020**, *15*, e0239369. [CrossRef]
29. Ahmed, T.A.; Aljaeid, B.M. Preparation, Characterization, and Potential Application of Chitosan, Chitosan Derivatives, and Chitosan Metal Nanoparticles in Pharmaceutical Drug Delivery. *Drug Des. Devel. Ther.* **2016**, *10*, 483–507. [CrossRef]